

One-Electron Oxidation and Reduction Potentials of Nitroxide Antioxidants: A Theoretical Study

Jennifer L. Hodgson,^{†,‡} Mansoor Namazian,^{†,‡} Steven E. Bottle,^{†,§} and Michelle L. Coote^{*,†,‡}

ARC Centre of Excellence for Free Radical Chemistry and Biotechnology, Research School of Chemistry, Australian National University, Canberra, ACT 0200, Australia, and Queensland University of Technology, Brisbane QLD 4000, Australia

Received: June 1, 2007; In Final Form: October 9, 2007

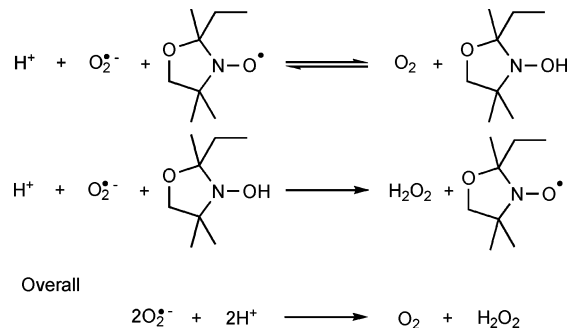
High-level ab initio calculations have been used to determine the oxidation and reduction potentials of a large number of nitroxides including derivatives of piperidine, pyrrolidine, isoindoline, and azaphenalene, substituted with COOH, NH₂, NH₃⁺, OCH₃, OH, and NO₂ groups, with a view to (a) identifying a low-cost theoretical procedures for the determination of electrode potentials of nitroxides and (b) studying the effect of substituents on these systems. Accurate oxidation and reduction potentials to within 40 mV (3.9 kJ mol⁻¹) of experimental values were found using G3(MP2)-RAD//B3-LYP/6-31G(d) gas-phase energies and PCM solvation calculations at the B3-LYP/6-31G(d) level. For larger systems, an ONIOM method in which G3(MP2)-RAD calculations for the core are combined with lower-cost RMP2/6-311+G(3df,2p) calculations for the full system, was able to approximate G3(MP2)-RAD values (to within 1.6 kJ mol⁻¹) at a fraction of the computational cost. The overall ring structure has more effect on the electrode potentials than the inclusion of substituents. Azaphenalene derivatives display the lowest oxidation potentials and least negative reduction potentials and are thus the most promising target to function as antioxidants in biological systems. Piperidine and pyrrolidine derivatives have intermediate oxidation potentials but on average pyrrolidine derivatives display more negative reduction potentials. Isoindoline derivatives show higher oxidation potentials and more negative reduction potentials. Within a ring, the substituents have a relatively small effect with electron donating groups such as amino and hydroxy groups stabilizing the oxidized species and electron withdrawing groups such as carboxy groups stabilizing the reduced species, as expected.

1. Introduction

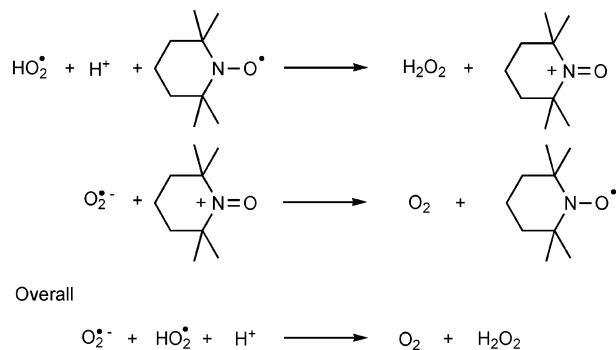
Cyclic nitroxide radicals, stabilized by bulky substituents, are persistent in tissues and in the circulatory system, and have been shown to be effective against radiation-induced damage in various experimental models. One way in which they are thought to protect against oxidative damage is derived from their ability to catalyze the dismutation of superoxide (O₂^{•-}), a toxic oxygen-derived species, by mimicking the activity of superoxide dismutase (SOD). The metal center in native SOD undergoes repeated reductions and oxidations allowing in catalytic fashion the dismutation of superoxide to oxygen and hydrogen peroxide.¹ In the case of 2-ethyl-2,5,5-trimethyl-3-oxazolidin-1-yloxy (OXANO) the nitroxide and its corresponding hydroxylamine react with superoxide independently of metal ions (Scheme 1).² In contrast, piperidine derivatives such as 2,2,6,6-tetramethylpiperidin-1-yloxy (TEMPO, **2**) undergo alternate oxidation and reduction reactions, because they are readily oxidized by protonated superoxide, [•]OOH, to yield the corresponding oxoammonium cation, which then oxidizes superoxide to molecular oxygen (Scheme 2).³

It is clear that the biological activity of nitroxides is linked to their electron-transfer rates and redox potentials. For six-membered cyclic nitroxides a direct correlation between oxidation potential and ability to protect from H₂O₂ induced oxidative damage has been observed.⁴ Because this trend is not repeated

SCHEME 1: SOD-Mimicking Behavior of OXANO



SCHEME 2: SOD-Mimicking Behavior of TEMPO



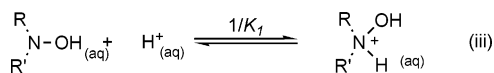
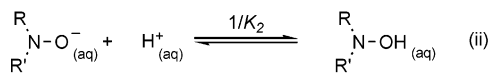
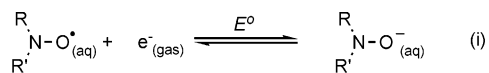
for the case of five-membered nitroxides, it is clear that additional factors contribute to their effectiveness; nonetheless, an understanding of substituent effects on electrode potentials is expected to assist in the determination of the roles nitroxides

* Author for correspondence. E-mail: mcoote@rsc.anu.edu.au.

[†] ARC Centre of Excellence for Free Radical Chemistry and Biotechnology.

[‡] Australian National University.

[§] Queensland University of Technology.

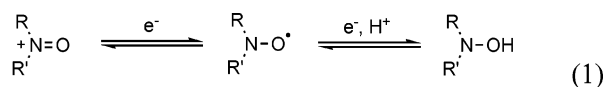
SCHEME 3: Suggested Mechanism for the Reduction of Nitroxides

play in biological systems. To this end, it would be useful to be able to predict the electrode potentials of a large number of nitroxide antioxidants via computational methods to study structures and substituents and eventually aid in the design of an optimal target for synthetic efforts.

Theoretical calculations of electrode potentials have previously been useful in the design of molecules with desirable redox properties, particularly for compounds where complex chemical equilibria are known to hamper experimental measurements.⁵ Successful calculation of electrode potentials requires accurate ab initio calculations of the enthalpy in the gas phase as well as accurate calculation of the differences in the free energy of solvation for each species.⁶ In this work a reliable computational method for the calculation of electrode potentials of nitroxides will be determined and used in the comparison of many different five and six-membered cyclic nitroxides.

2. Electrode Potentials

Nitroxide radicals can be reversibly oxidized to the corresponding oxoammonium cation by various chemical and electrochemical means.



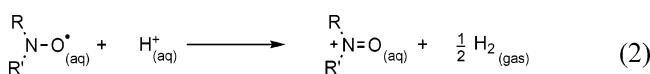
oxoammonium cation

nitroxide radical

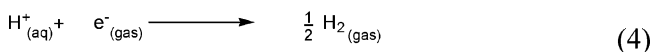
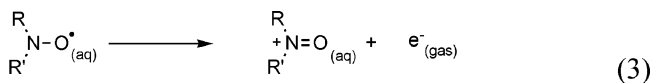
hydroxylamine

Reduction of a nitroxide is known to produce a hydroxylamine; however, there has been some debate over the mechanism of this process. Fish et al.⁷ suggest a reaction scheme for reduction in which a one-electron reduction is followed by two reversible protonation steps (see Scheme 3). Thus for comparison with experimental values in solution, the acid dissociation constants of these protonation steps, K_1 and K_2 , need to be calculated as well as the formal potential of the electron-transfer process, E° .

Two different methodological approaches can be used for the calculation of redox potentials in solution.⁸ One method is to use an isodesmic reaction to calculate the Gibbs energy of the reaction relative to a reference system. Results for this method have been shown to be somewhat dependent upon the reference molecule used,⁹ limiting the predictive power of this method. A second approach, in which electrons and protons are used explicitly as the reference system for the reactions, will be used here and is described as follows. For the nitroxides standard oxidation potentials are calculated relative to the SHE (standard hydrogen electrode) by determining the Gibbs free energy of the following reaction:



The Gibbs energy change of reaction (2) can be written in terms of these two-half-reactions:



The standard Gibbs energy is then the sum of the Gibbs energies of reactions 3 and 4.

$$\Delta G_2^\circ = \Delta G_3^\circ + \Delta G_4^\circ \quad (5)$$

The Gibbs free energy of reaction 4, ΔG_4° , is reported to be -4.36 eV,⁵ and the value of ΔG_3° can be obtained from the calculated Gibbs energy of each component in the reaction. This requires the gas-phase energy of each component, $\Delta G_{i,\text{gas}}^\circ$, together with its solvation energy, $\Delta G_{i,\text{solv}}^\circ$.

$$\Delta G_3^\circ = \sum v_i \Delta G_i^\circ \quad (6)$$

$$\Delta G_i^\circ = \Delta G_{i,\text{gas}}^\circ + \Delta G_{i,\text{solv}}^\circ \quad (7)$$

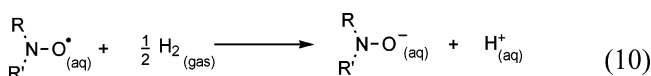
The oxidation potential can then be obtained using the following equation,¹⁰ where n is the number of electrons transferred (in this case $n = 1$), and F is the Faraday constant (96485.3383 coulombs/mol):

$$\Delta G_2^\circ = nFE_{\text{ox}}^\circ \quad (8)$$

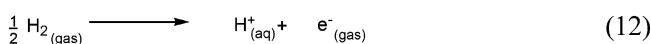
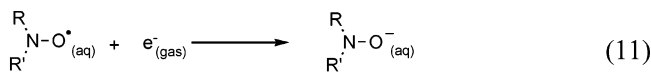
As noted above, the mechanism for reduction leading to a hydroxylamine is more complicated than a simple one-electron-transfer reaction. In a study by Kato et al.¹¹ the relationship between the formal potential of the electron-transfer process, E° , and the acid dissociation constants, K_1 and K_2 , was investigated for a range of pH values and the relationship between these values and the experimentally determined reversible half-wave potential, $E_{1/2}^{\text{rev}}$, was found to be

$$E_{1/2}^{\text{rev}} = E^\circ - \frac{RT}{F} \ln(K_1 K_2) + \frac{RT}{F} \ln(K_1 K_2 + K_1 [\text{H}^+] + [\text{H}^+]^2) \quad (9)$$

This relationship was also reported subsequently by Israeli et al.¹² In the present work only two relatively simple cases will be compared directly with experimental data using this equation. However, for the study of structure reactivity trends, a simpler approach will be adopted in which a one-electron-transfer similar to that used for the oxidation potentials will be used to calculate the reduction potential of each molecule with respect to the SHE. In this case the Gibbs energy change is measured by the reaction:



with the two-half reactions:



The reduction potential is found using⁹

$$\Delta G_{10}^{\circ} = \Delta G_{11}^{\circ} + \Delta G_{12}^{\circ} \quad (13)$$

$$\Delta G_{10}^{\circ} = -nFE_{\text{red}}^{\circ} \quad (14)$$

3. Theoretical Procedures

Standard ab initio molecular orbital¹³ and density functional¹⁴ calculations in this work were carried out using GAUSSIAN 03¹⁵ and MOLPRO 2000.6.¹⁶ Calculations on radicals were performed with an unrestricted wave function except in cases designated with an “R” prefix where a restricted open-shell wave function was used. It should be noted that all radicals and all closed-shell species considered in this study were true (local) minimum energy structures (i.e., having no imaginary frequencies).

To find a suitable low-cost procedure with which to model the larger systems in this study, the performance of a variety of levels of theory was assessed for several relatively small nitroxides for which experimental ionization energies and electrode potentials have been determined. Geometries of the neutral radicals as well as the positively and negatively charged species were optimized using various wavefunctions and basis sets and the results were benchmarked against the high-level QCISD/6-31G(d) method. To assess the effect of the level of theory used for geometry optimization on the resulting ionization energies and electron affinities, single point energy calculations were carried out on all the geometries at the QCISD/6-31G(d) level.

Adiabatic ionization energies and electron affinities for several nitroxides, using species optimized at the B3-LYP/6-31G(d) level, were calculated at a wide variety of levels of theory, ranging from relatively low-cost DFT and MP2 methods to computationally expensive high-level composite methods from the G3 family (G3, G3X, G3(MP2), G3X(MP2), and their “RAD” variants).^{17,18} These composite methods attempt to approximate either CCSD(T) or QCISD(T) energies with a large triple- ζ basis set via additivity approximations carried out at the MP2 and/or MP4 levels of theory. As the accuracy of the G3 family is dependent upon the method used and also the system examined, G3 calculations with the “X” and “RAD” variation as well as the “MP2” approximation were made.

Ionization energies and electron affinities were also calculated using versions of the ONIOM¹⁹ method. We have previously shown that this method is suitable for radical reactions,^{20,21} and in the present work examine its suitability for calculating the electrode potentials of nitroxides. In ONIOM, a chemical reaction is divided into a core section that includes the reaction center and principal substituents, and an outer section, which is the rest of the chemical system. The core system is calculated at a high level of theory and also at a lower level of theory, and the full chemical system is calculated only at the lower level. In forming the core section, deleted substituents are replaced with link atoms, typically hydrogens, so that the correct valency is maintained and the core provides a good model of the chemical reaction under study. The energy of the whole chemical system is then obtained as the sum of the high-level energy for the core system, and the substituent effect of the outer section calculated at the lower level. This approximation is exact if the low level of theory measures the substituent effect accurately. In the present work, two lower-cost methods were tested for this purpose, RMP2/6-311+G(3df,2p) and B3-LYP/6-311+G(3df,2p), and G3(MP2)-RAD was the high level of theory used to study the core section. As in the case of other calculations in this study, geometries were optimized at the B3-LYP/6-31G(d) level of theory.

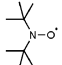
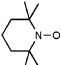
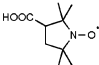
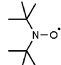
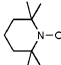
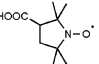
The free energy of solvation of the neutral and charged species is expected to contribute to the calculated of electrode potentials in aqueous medium. The effect of method and basis set on the polarized continuum models PCM²² and CPCM²³ were assessed, with the molecular structures re-optimized in a water medium as implemented in the GAUSSIAN 03 package. The recommended radii were used for these calculations, i.e., the united atom topological model applied on radii optimized for the HF/6-31G(d) and PBE0/6-31G(d) levels of theory were used for the Hartree–Fock and B3-LYP methods, respectively.²⁴ The free energies of solvation were added to the gas-phase ionization energies calculated at the G3(MP2)-RAD//B3-LYP/6-31G(d) level to convert them to oxidation potentials for comparison with experimental results. The reduction potentials of various nitrogen oxides have been calculated via similar methods and have been found to correlate to experimental data with an average error of 120 mV for both the PCM and CPCM models.²⁵

Having determined a suitable computational method, the oxidation and reduction potentials of many differently substituted nitroxides including derivatives of piperidine, pyrrolidine, isoindoline, and azaphenalene were calculated. The geometries of the neutral and charged species were optimized at the B3-LYP/6-31G(d) level of theory. Frequency calculations were also carried out at the B3-LYP/6-31G(d) level and scaled via the appropriate factors.²⁶ Significant effort was taken to ensure that the optimized structure was the global (rather than merely the local) minimum energy structure by performing extensive conformational searches at the same level. Improved gas-phase energies were obtained via G3(MP2)-RAD calculations on the B3-LYP optimized structures. An ONIOM approximation that combined G3(MP2)-RAD calculations for the core and RMP2/6-311+G(3df,2p) calculations for the full system was used for larger systems. The solvation energies of each species were calculated using the polarized continuum model PCM at the B3-LYP/6-31G(d) level and added to the gas-phase free energies to give the total Gibbs energies of the species. The oxidation and reduction potentials were then found using eqs 8 and 14.

4. Results and Discussion

Assessment. To identify an appropriate low-cost method for obtaining geometries, optimizations were carried out at a variety of levels of theory from computationally lower-cost HF and DFT methods to more demanding MP2 and QCISD calculations, with both small and larger basis sets. In the present work we are only concerned with whether potential errors in the geometry of species lead to errors in the calculated electrode potentials. Therefore, to establish whether differences in the procedure used to optimize geometry will have any significant effect on the electrode potentials for the nitroxide systems studied here, single point energies in the gas phase were calculated at a consistent level of theory (QCISD/6-31G(d)) for various optimized geometries of the neutral, positively and negatively charged nitroxides (see Table 1). In line with earlier studies showing that low-cost methods perform very well in geometry optimizations of nitroxides,²⁷ it can be seen that all of the low-cost methods yield reasonably accurate geometries, though there are some minor differences among the methods used. For the present systems, the DFT method B3-LYP/6-31G(d) appears to offer the best compromise between accuracy and computational cost and has therefore been adopted for the determination of the geometries of species in this study. The ionization energies and electron affinities, calculated using B3-LYP/6-31G(d) optimized geometries show a difference of less than 0.004 eV from the corresponding benchmark values.

TABLE 1: Effect of Level of Theory Used for Geometry Optimization on the Adiabatic Ionization Energies and Electron Affinities (0 K, Expressed in eV) of Nitroxides^a

Level of theory	Ionization energy			Electron affinity		
						
HF/6-31G(d)	6.45	6.51	6.62	-0.63	-0.60	-0.53
HF/6-311+G(2d)	6.48	6.54	6.65	-0.64	-0.62	-0.55
HF/6-311+G(3df,2p)	6.48	6.54	6.66	-0.64	-0.62	-0.55
B3-LYP/6-31G(d)	6.39	6.45	6.56	-0.62	-0.59	-0.52
B3-LYP/6-311+G(2d)	6.40	6.46	6.57	-0.63	-0.61	-0.53
B3-LYP/6-311+G(3df,2p)	6.40	6.46	6.57	-0.63	-0.61	-0.53
B3-LYP/cc-pVDZ	6.39	6.46	6.57	-0.62	-0.60	-0.52
B3-LYP/cc-pVTZ	6.40	6.46	6.57	-0.62	-0.59	-0.52
MP2/6-31G(d)	6.41	6.47	6.59	-0.61	-0.58	-0.51
MP2/6-311+G(d)	6.40	6.45	6.57	-0.63	-0.60	-0.53
MP2/6-311+G(3df,2p)	6.40	6.46	-	-0.61	-0.59	-
QCISD/6-31G(d)	6.39	6.45	-	-0.62	-0.59	-

^a Found from single point energy calculations at the QCISD/6-31G(d) level for species optimized using various wavefunctions and basis sets.

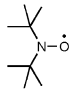
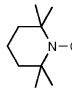
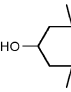
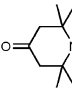
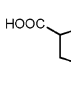
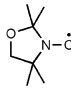
To assess the effect of level of theory on the energetics, the adiabatic ionization energies of several common nitroxides were calculated at a variety of levels of theory using the B3-LYP/6-31G(d) geometries (Table 2). Their corresponding electron affinities were also calculated and are shown in Table 3. Experimental ionization energies are available for TEMPO (2) and di-*tert*-butyl nitroxide (DBN, 1);²⁸ however, the temperature at which these experiments were carried out is unclear. The results may therefore deviate from the 0 K values calculated in the present work by a small thermal correction. Taking this into consideration, calculations performed at the highest levels of theory compare reasonably well with experimental data. More generally, the G3 levels of theory are known to deliver “chemical accuracy” (within approximately 1 kcal mol⁻¹) in comparison with the G2/97 test set of experimental data^{17,18} and are treated as benchmark values for the remainder of this work. Among the various types of G3 methods tested, all produced ionization energies and electron affinities within 0.04 eV of each other. The method G3(MP2)-RAD is selected as an appropriate high-level method to use for further studies on these systems because it is the lowest-cost G3 method that includes the “RAD” variant, especially designed to deal with open-shell species.¹⁸ Therefore, in Tables 2 and 3, MADs were calculated using this method as a benchmark.

Various low-cost DFT and MP2 procedures were also examined with a view to finding a suitable method to use for larger systems for which G3(MP2)-RAD calculations would be impractical. Traditionally, single point energies calculated using either DFT^{5,10,29} or MP2³⁰ procedures have been adopted as low-cost methods for calculating electrode potentials. However, from Tables 2 and 3, it is clear that in the present systems all of these methods produce values that vary considerably from the benchmark G3 values and would not be suitable as accurate low-cost methods. Recently, we have had considerable success using an ONIOM method to approximate G3(MP2)-RAD

energies at a fraction of the computational cost.²¹ To test the accuracy of this approach in the present reactions, we therefore also calculated the ionization energies and electron affinities using a version of ONIOM in which the core of the reaction was calculated using either RMP2/6-311+G(3df,2p) or B3-LYP/6-311+G(3df,2p). The core reaction was obtained by deleting all substituents beyond the β -position to the radical center and replacing them with methyl groups, leaving the core reaction in all cases as the oxidation or reduction of the smaller radical $\cdot\text{ON}(\text{C}(\text{CH}_3)_3)_2$, known as di-*tert*-butyl nitroxide (DBN, 1). From Tables 2 and 3 it is clear that the ionization energies and electron affinities obtained using these two versions of the ONIOM method show excellent agreement with the G3(MP2)-RAD values, with the best results obtained when the substituent effect is measured using RMP2/6-311+G(3df,2p). In this latter case the MADs, relative to full G3(MP2)-RAD calculations, are only 0.017 eV (1.6 kJ mol⁻¹). Of course, treating the entire ring structure of the system as a complete functional group and including it intact in the core reaction would achieve an even better approximation to the full system. Although this adds to the computational cost, such calculations remain practical for the nitoxides examined in the present work and thus the parent (H-substituted) ring structure will be used as the core system for the larger systems in this study.

The effect of level of theory, basis set and solvation model used to calculate the free energy of solvation of molecules in the study was also assessed. The results are shown in Table 4. As no experimental values of the solvation energies of nitroxides are available, the calculated free energies of solvation were added to the gas-phase energies calculated at the G3(MP2)-RAD//B3-LYP/6-31G(d) level to transform them into oxidation potentials using eqs 2–8, for direct comparison with experimental values. The results show that the oxidation potentials vary only a small amount with the different methods of calculating solvation energy. The MADs of the methods vary

TABLE 2: Effect of Level of Theory on the Adiabatic Ionization Energies (0 K, Expressed in eV) of Various Nitroxides^a

Level of Theory							MAD ^b
B3-LYP/6-311+G(3df,2p)	6.91	6.97	7.07	7.36	7.15	7.28	0.075
MPW1K/6-311+G(3df,2p)	7.04	7.10	7.20	7.50	7.27	7.41	0.205
MPW1B95/6-311+G(3df,2p)	6.80	6.86	6.96	7.24	7.01	7.15	0.045
MPWB1K/6-311+G(3df,2p)	6.89	6.95	7.04	7.34	7.10	7.25	0.047
RMP2/6-311+G(3df,2p)	6.70	6.76	6.85	7.09	6.94	7.08	0.146
UCBS-QB3	7.21	6.89	6.98	7.25	7.03	7.17	0.078
CBS-QB3	7.21	6.90	6.99	7.26	7.04	7.18	0.074
G3(MP2)	6.83	6.90	6.99	7.26	7.04	7.17	0.017
G3X(MP2)	6.82	6.89	6.99	7.25	7.03	7.16	0.026
G3(MP2)-RAD	6.85	6.91	7.01	7.27	7.06	7.19	0
G3X(MP2)-RAD	6.85	6.91	7.01	7.27	7.06	7.19	0.000
G3	6.81	6.88	6.98	7.24	-	7.16	0.030
G3X	6.81	6.88	6.97	7.24	-	7.15	0.034
ONIOM (RMP2) ^c	6.85	6.91	6.99	7.23	7.08	7.22	0.017
ONIOM (B3-LYP) ^d	6.85	6.90	7.02	7.31	7.09	7.22	0.021
Experimental	6.77	6.73	-	-	-	-	-

^a Calculated using species optimized at the B3-LYP/6-31G(d) level with the B3-LYP/6-31G(d) zero point vibrational energy. ^b Mean absolute deviation from the benchmark G3(MP2)-RAD value. This level was used as the benchmark rather than experimental values or a higher level of theory as we have a full set of values for comparison and use this level for further calculations in the study. ^c Found using core systems of $\cdot\text{ON}(\text{C}(\text{CH}_3)_3)_2$ and $\text{O}=\text{N}^+(\text{C}(\text{CH}_3)_3)_2$ calculated at G3(MP2)-RAD, with the full system calculated at RMP2/6-311+G(3df,2p). ^d Found using core systems of $\cdot\text{ON}(\text{C}(\text{CH}_3)_3)_2$ and $\text{O}=\text{N}^+(\text{C}(\text{CH}_3)_3)_2$ calculated at G3(MP2)-RAD, with the full system calculated at B3-LYP/6-311+G(3df,2p).

13 mV (1.2 kJ mol⁻¹) from each other and are only around 35 mV (3.4 kJ mol⁻¹) from the experimentally determined values.

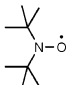
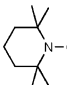
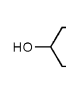
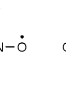
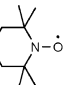
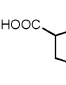
As level of theory, basis set, and solvation model are shown to have very little effect on the value of the free energy of solvation, the method chosen for use in this study appears to be fairly arbitrary. A PCM solvation model was chosen, as it has been shown that the maximum deviation of calculated values from experimental data is less than that found using CPCM for a range of nitrogen oxides.²⁵ As geometries are reoptimized during the solvation energy calculation, a B3-LYP level was chosen, as it has been shown to be more reliable for geometry optimizations (see Table 1). From Table 4 it is seen that the MAD is lowered by the use of the SCFVAC keyword in the GAUSSIAN calculation. This keyword effectively adds a small solute polarization term to the free energy of solvation by performing the SCF calculation both with and without the presence of the solvent field (see footnotes to Table 4).²⁴ Finally, it is noted that the use of a larger basis set actually increased the MAD, probably due to the fact that the (semiempirical) solvation models are parametrized to the 6-31G(d) basis set. Therefore a suitable method for the calculation of free energy of solvation for nitroxides is the PCM model at the B3-LYP/6-31G(d) level using an SCFVAC keyword in the GAUSSIAN calculation.

In summary, G3(MP2)-RAD//B3-LYP/6-31G(d) is an appropriate level of theory for the calculation of one electron oxidation and reduction potentials of nitroxides, with the ONIOM method providing a good approximation to it for large

systems. The electrode potentials are relatively insensitive to the solvation model, and the PCM model at the B3-LYP/6-31G(d) level seems the most appropriate method. Using these methods oxidation potentials can be compared to experimental results^{12,31} (Figure 1). The ab initio and experimental results compare very well, with only one outlying point for the species 4-hydroxy-TEMPO (**6**). The other species show a mean average deviation of 23 mV (2.2 kJ mol⁻¹) from the experimental results with a maximum deviation of 40 mV (3.9 kJ mol⁻¹).

As explained above, the reduction of nitroxides is thought to be more complex than simply the reverse of the one-electron oxidation, with a multiple step reaction mechanism⁷ (shown in Scheme 3). Half-wave potentials of reduction comparable to experimental values were therefore calculated according to eq 9 for both TEMPO (**2**) and 4-hydroxy-TEMPO (**6**). The reduction potential, E° , was found using the previously described method to calculate eq 14. The G3(MP2)-RAD//B3-LYP/6-31G(d) gas-phase energies and PCM (at the B3-LYP/6-31G(d) level) solvation energies for the nitroxide species in reactions ii and iii of Scheme 3 were transformed to acid dissociation constants, K_1 and K_2 , using the method of Liptak and Shields,³² in which the experimental values of the gas-phase energy (-6.28 kcal mol⁻¹) and free energy of solvation (-264.61 kcal mol⁻¹) of H⁺ are included, to calculate pK_a values. Using the determined values of E° , K_1 , and K_2 , the half-wave potentials of molecules **2** and **6** were calculated using eq 9, at room temperature and pH 7 ([H⁺] = 10⁻⁷), to be -31 and -11 mV, respectively, versus a saturated calomel reference

TABLE 3: Effect of Level of Theory on the Adiabatic Electron Affinities (0 K, Expressed in eV) of Various Nitroxides^a

Level of Theory							MAD ^b
B3-LYP/6-311+G(3df,2p)	0.29	0.31	0.49	0.71	0.44	0.41	0.229
MPW1K/6-311+G(3df,2p)	0.08	0.12	0.29	0.53	0.21	0.21	0.432
MPW1B95/6-311+G(3df,2p)	0.16	0.22	0.39	0.62	0.32	0.29	0.336
MPWB1K/6-311+G(3df,2p)	0.09	0.15	0.32	0.56	0.23	0.22	0.408
RMP2/6-311+G(3df,2p)	0.41	0.46	0.65	0.88	0.51	0.51	0.103
UCBS-QB3	0.10	0.52	0.69	0.91	0.59	0.60	0.104
CBS-QB3	0.09	0.51	0.69	0.90	0.59	0.59	0.110
G3(MP2)	0.55	0.59	0.77	0.98	0.68	0.67	0.037
G3X(MP2)	0.55	0.59	0.77	0.98	0.68	0.67	0.035
G3(MP2)-RAD	0.52	0.56	0.74	0.95	0.63	0.63	0
G3X(MP2)-RAD	0.52	0.56	0.74	0.96	0.64	0.64	0.003
G3	0.53	0.57	0.75	0.96	-	0.66	0.016
G3X	0.53	0.58	0.76	0.97	-	0.66	0.021
ONIOM (RMP2) ^c	0.52	0.57	0.76	0.99	0.62	0.62	0.017
ONIOM (B3-LYP) ^d	0.52	0.54	0.72	0.95	0.68	0.65	0.017

^a Calculated using species optimized at the B3-LYP/6-31G(d) level with the B3-LYP/6-31G(d) zero point vibrational energy. ^b Mean absolute deviation from the benchmark G3(MP2)-RAD value. This level was used as the benchmark rather than experimental values or a higher level of theory as we have a full set of values for comparison and use this level for further calculations in the study. ^c Found using core systems of $\cdot\text{ON}(\text{C}(\text{CH}_3)_3)_2$ and $\text{ON}(\text{C}(\text{CH}_3)_3)_2^-$ calculated at G3(MP2)-RAD, with the full system calculated at RMP2/6-311+G(3df,2p). ^d Found using core systems of $\cdot\text{ON}(\text{C}(\text{CH}_3)_3)_2$ and $\text{ON}(\text{C}(\text{CH}_3)_3)_2^-$ calculated at G3(MP2)-RAD, with the full system calculated at B3-LYP/6-311+G(3df,2p).

electrode (SCE). Reported experimental values for the same are -37 and -16 mV,¹¹ showing agreement to within 10 mV (1.0 kJ mol⁻¹). A subsequent study reported the half-wave potentials of reduction for the same species versus the standard hydrogen electrode (SHE).¹² Using eq 9, our calculated half-wave potentials versus SHE of molecules **2** and **6** were found to be 213 and 233 mV, respectively (again at room temperature and pH 7), which are in good agreement with the corresponding experimental values (estimated from Figure 6 in ref 12 to be approximately 200 mV in each case).

Structure–Reactivity Trends. Having identified a reliable computational method, the oxidation and reduction potentials were able to be calculated for a large number of nitroxides including di-*tert*-butyl nitroxide (DBN, **1**), many derivatives of 2,2,6,6-tetramethylpiperidin-1-yloxy (TEMPO, **2**), 2,2,5,5-tetramethylpyrrolidin-1-yloxy (PROXYL, **14**), 1,1,3,3-tetramethylisoindolin-2-yloxy (TMIO, **23**), and 1,1,3,3-tetramethyl-2,3-dihydro-2-azaphenalene-2-yloxy (TMAO, **36**), as well as one example of an oxazolidine (2,2,5,5-tetramethyl-3-oxazolidin-1-yloxy, **22**). The results are shown in Table 5 and Figure 2.

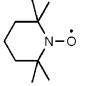
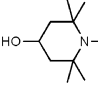
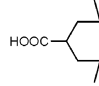
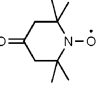
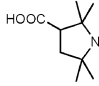
From Figure 2 the order of increasing favorability for the reduction potentials of the parent (H-substituted) species is PROXYL (**14**), DBN (**1**), TMIO (**23**), TEMPO (**2**), 2,2,5,5-tetramethyl-3-oxazolidin-1-yloxy (**22**), and TMAO (**36**). In general, the five-membered cyclic nitroxides (pyrrolidine and isoindoline derivatives) have reduction potentials centered around -1570 mV, and the six-membered cyclic nitroxides (piperidine and azaphenalene derivatives) have reduction potentials around 200 mV less negative, centered at -1370 mV.

The order for the oxidation potentials of the parent compounds is not the inverse of the results for the reduction potentials but instead follows the order of increasing favorability, 2,2,5,5-tetramethyl-3-oxazolidin-1-yloxy (**22**), TMIO (**23**), PROXYL (**14**), TEMPO (**2**), DBN (**1**), and TMAO (**36**). In general, the lowest oxidation potentials are seen for the azaphenalene derivatives centered around 510 mV and the highest for the isoindoline derivatives centered around 1020 mV. Piperidine and pyrrolidine derivatives show oxidation potentials centered around 830 mV.

The oxazolidine derivative, **22**, is easily reduced but not very easily oxidized, because the electronegative oxygen stabilizes the negative charge over the ring when the anion is formed but destabilizes the positive charge when the cation is formed. This is consistent with the observation that the very similar species OXANO undergoes reduction to the corresponding hydroxylamine, with the reduced species then being reoxidized back to the nitroxide radical, in the SOD-mimicking reaction seen in Scheme 1.² In contrast, nitroxides such as the piperidine derivatives in this study are thought to undergo oxidation to the corresponding oxoammonium cation, with the oxidized species then undergoing reduction, as seen in Scheme 2.³

The ability of the cyclic nitroxides studied here to be oxidized or reduced appears to be related to the flexibility of the ring structure, which determines how easily the anion is pyramidalized and the cation is planarized at the nitrogen center. The noncyclic DBN (**1**) can be planarized easily, but steric hindrance between the methyl groups causes the pyramidal anion to be of higher energy. Therefore DBN shows a lower oxidation

TABLE 4: Effect of Level of Theory, Basis Set and Solvation Model Used to Calculate the Free Energy of Solvation, on the Oxidation Potentials (298 K, Expressed in mV) of Various Nitroxides^a

Method	Basis Set	Solvation Model ^b	Oxidation potential					MAD ^c
								
HF	6-31G(d)	PCM	784.3	772.6	781.1	896.0	886.1	31.7
		CPCM	784.0	771.6	780.1	893.8	895.2	34.3
	6-311+G(3df,2p)	PCM	807.7	785.7	788.8	890.8	909.2	37.9
		CPCM	807.9	784.4	784.3	891.5	911.1	39.4
B3-LYP	6-31G(d)	PCM	794.4	780.8	813.1	939.6	928.3	37.3
		PCM ^{†d}	762.1	756.4	793.7	946.1	909.9	34.0
		CPCM	793.8	778.5	809.7	934.8	926.7	35.7
	6-311+G(3df,2p)	PCM	819.9	798.6	813.3	940.3	953.4	44.1
		CPCM	820.8	798.6	810.1	939.7	954.3	43.7
		Experimental ^e	740	825	805	918	870	0

^a Calculated using gas-phase species optimized at the G3(MP2)-RAD level with B3-LYP/6-31G(d) optimized geometries. ^b Calculated using the united atom topological model with the recommended optimization of radii, i.e., UAHF and UAKS keywords for the Hartree-Fock and B3-LYP methods, respectively.²¹ ^c Mean absolute deviation from the experimental values. ^d Calculated using the SCFVAC keyword in GAUSSIAN. SCFVAC allows for the calculation of the Gibb's free energy of solvation because an additional SCF calculation is performed in the absence of the solvent field, so as to find $\langle \psi(0)|H|\psi(0) \rangle$ (where $\psi(0)$ is the wavefunction in the gas phase). When this keyword is not used, the Gibb's free energy of solvation is instead estimated as the difference of $\langle \psi(f)|H|\psi(f) \rangle$ (where $\psi(f)$ is the wavefunction in the presence of the solvent field) and the total Gibb's free energy of the solute in solution. The difference between $\langle \psi(0)|H|\psi(0) \rangle$ and $\langle \psi(f)|H|\psi(f) \rangle$ is a small solute polarization term, which is added to the electrostatic component of the total free energy of solvation when the SCFVAC keyword is used and omitted when it is not.²⁴ ^e As reported by Goldstein et al.³¹ and Israeli et al.¹²

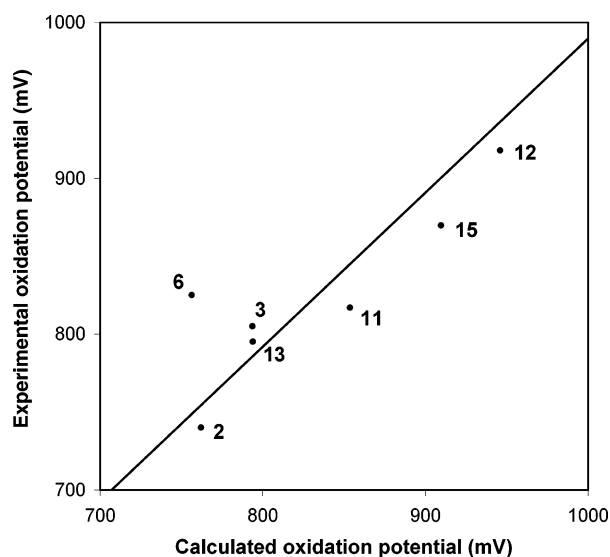
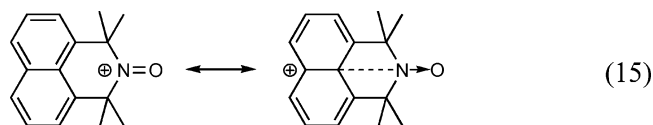


Figure 1. Experimental oxidation potentials versus calculated values from the present work.^{12,31} Corresponding structure numbers can be found in Table 5.

potential, but a more negative reduction potential. All other things being equal piperidine and pyrrolidine rings are relatively flexible, with out-of-plane motion that has in the past been studied using quantum mechanical methods.²⁷ Piperidine derivatives are more easily reduced, indicating that they are more easily pyramidalized around the nitrogen center in the anion form, however the similar oxidation potentials of piperidines and pyrrolidines indicates that they are both relatively easy to

planarize in the cation form. On the other hand, the five-membered ring in the isoindoline derivatives is held quite rigid by the presence of an aromatic ring, leading to higher oxidative potentials and more negative reductive potentials for these species. This is demonstrated through the observation that the isotropic EPR spectra of the TMIO family of radicals have line widths much smaller than those of the TEMPO family of radicals.^{33,34} Despite the presence of two fused aromatic rings, the six-membered ring in azaphenylene is quite flexible around the nitrogen center, showing similar steric characteristics to TEMPO-like nitroxides in the vicinity of the nitroxide group. The EPR spectrum of TMAO (**36**) confirms this, showing broader lines than the spectra of the TMIO family.³⁵

Azaphenylene derivatives show even lower oxidation potentials than piperidines due to the fact that the positive charge in the cation species can be delocalized onto the ring by hyperconjugation.



Azaphenolens are more easily oxidized than other nitroxides and at the same time relatively easily reduced. They should therefore undergo relatively fast one-electron redox based processes such as SOD-mimicking reactions, making them an interesting target to test for their protecting ability against oxidative damage.

For all of the different types of ring structures studied, trends in the oxidation and reduction potentials within a family are in

TABLE 5: Electrode Potentials (Calculated at 298 K) of Nitroxides Compared to the Standard Hydrogen Electrode (SHE) in an Aqueous Medium^a

Entry	Nitroxide	Oxidation potential (mV)	Reduction potential (mV) ^c	Entry	Nitroxide	Oxidation potential (mV)	Reduction potential (mV) ^c
1		696.5	-1552.9	28 ^b		1024.2	-1935.5
2		762.1	-1482.5	29 ^b		1016.2	-1697.2
3		793.7	-1387.6	30 ^b		1022.9	-2331.0
4		703.7	-1455.3	31 ^b		1072.2	-1754.7
5		779.8	-1436.3	32 ^b		1106.5	-1616.7
6		756.4	-1413.5	33 ^b		1056.6	-1423.7
7 ^b		741.3	-1783.3	34 ^b		965.2	-1497.5
8		878.5	-1347.9	35 ^b		1100.3	-1757.6
9 ^b		914.0	-1270.0	36		469.1	-1336.0
10 ^b		1016.1	-1217.1	37 ^b		481.0	-1313.4
11		853.8	-1315.2	38 ^b		529.8	-1390.5
12		946.1	-1255.1	39 ^b		512.7	-1355.6
13		793.9	-1479.5	40 ^b		486.1	-1328.4
14		763.7	-1621.3	41 ^b		527.2	-1475.4
15		909.9	-1504.8	42 ^b		510.8	-1792.0
16		729.5	-1591.4	43 ^b		554.2	-1542.6
17		726.9	-1552.6	44 ^b		509.6	-1226.3
18		718.5	-1598.0	45 ^b		619.2	-1402.0

TABLE 5 (Continued)

Entry	Nitroxide	Oxidation potential (mV)	Reduction potential (mV) ^c	Entry	Nitroxide	Oxidation potential (mV)	Reduction potential (mV) ^c
19 ^b		765.3	-1722.8	46 ^b		593.4	-1468.2
20 ^b		997.2	-1396.0	47 ^b		601.1	-1384.2
21		1043.9	-	48 ^b		540.7	-1328.7
22		1023.0	-1349.6	49 ^b		386.7	-1317.9
23		1000.3	-1504.8	50 ^b		439.9	-1346.7
24 ^b		1055.7	-1536.8	51 ^b		359.2	-1369.0
25 ^b		941.7	-1525.7	52 ^b		575.2	-1449.6
26 ^b		974.4	-1544.0	53 ^b		555.0	-2236.5
27 ^b		971.0	-1516.0	54 ^b		514.0	-2343.1

^a Calculated using gas-phase species optimized at the G3(MP2)-RAD level with B3-LYP/6-31G(d) optimized geometries. Solvation energies were calculated using PCM at the B3-LYP/6-31G(d) level of theory using the SCFVAC keyword in GAUSSIAN. ^b ONIOM calculations found using core systems calculated at G3(MP2)-RAD, with the full system calculated at RMP2/6-311+G(3df,2p); using as core systems the parent (H-substituted) nitroxides. i.e., **2** is the core system for **7** and **9**, **10** and **14** are the core systems for **19** and **20**, **23** is the core system for **24–35**, and **36** is the core system for **37–54**. ^c Note that this is the formal one electron reduction reductional potential. For comparison with the experimental irreversible half-wave potentials, the protonation of the reduced species would need to be taken into account, as per eq 9. As noted above, this has been done for TEMPO (**2**) and 4-hydroxy-TEMPO (**6**), and the resulting the half-wave potentials (versus SHE at room temperature and pH 7) are 213 and 233 mV, respectively.

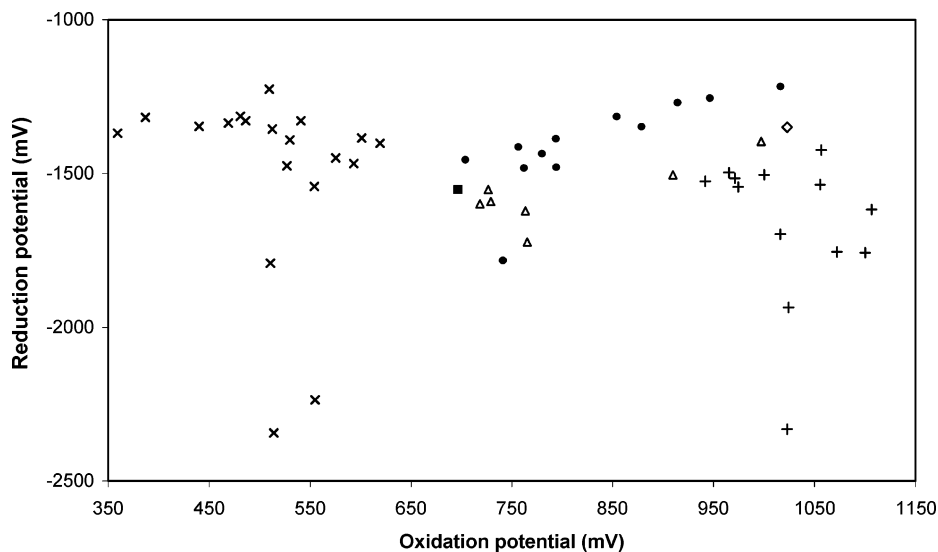


Figure 2. Plot of the relationship between oxidation and reduction potentials of nitroxides: di-*tert*-butyl nitroxide (■); piperidine derivatives (●); pyrrolidine derivatives (△); oxazolidine derivatives (◇); isoindoline derivatives (+); azaphenalene derivatives (×).

line with the electron donating and accepting abilities of the ring substituents. The piperidine and pyrrolidine derivatives show oxidation potentials that increase with substituents in the

order NH₂, OH, OCH₃, COOH, and NH₃⁺, but the reduction potentials become less negative with the same substituents. As expected, the increase in electron density around the ring from

donating substituents stabilizes the positive charge in the oxidized species, and substituents with a greater electron accepting ability stabilize the negative charge in the reduced ring. However, these effects are observed to be relatively small. For instance, in the sequence of substituted TEMPO radicals, nitroxides substituted in the 4-position with neutral substituents (H, COOH, NH₂, OCH₃, and OH) show an oxidation potential that varies by only 90 mV, whereas there are several hundred millivolts between the parent (H-substituted) species themselves.

Substituent effects in the isoindoline and azaphenalene derivatives largely follow electronegativity trends with, for example, NH₂ stabilizing the cation and lowering the oxidation potential and COOH stabilizing the anion and making reduction more favorable. However, some variation occurs with the substituent position around the rings, possibly due to the way in which charge can be delocalized via hyperconjugation. Some functional groups around the ring may accept large proportions of negative charge, further complicating these effects. Other factors such as steric effects may also contribute, for example, the species 4,7-dicarboxy-TMIO (**30**) shows hydrogen bonding in the neutral radical, which is disrupted in the cation and anion species, leading to the relatively unfavorable oxidation and reduction potentials observed for this species. Overall, however, with a few minor exceptions, the electrode potentials of the nitroxides are not very sensitive to substituents. This may be a useful feature in the design of new targets for synthetic efforts as it is expected that substituents can be chosen to affect other properties of a nitroxide such as its solubility or binding without significantly compromising its antioxidant ability.

5. Conclusions

The calculation of electrode potentials for nitroxide antioxidants was investigated and the computational method G3(MP2)-RAD//B3-LYP/6-31G(d) with PCM solvation energies at the B3-LYP/6-31G(d) level was found to be suitable for these molecules, giving oxidation and reduction potentials within 40 mV (3.9 kJ mol⁻¹) of experimental values. An ONIOM-based approach in which the core, modeled as the reaction of the small radical *ON(C(CH₃)₃)₂, was studied at G3(MP2)-RAD and the substituent effect of the full system was calculated at RMP2/6-311+G(3df,2p), was shown to provide an accurate lower-cost alternative method for larger systems. This method was able to approximate G3(MP2)-RAD values (to within 1.6 kJ mol⁻¹) at a fraction of the computational cost.

Calculations on a wide range of cyclic nitroxide species showed that oxidation and reduction potentials are strongly affected by the ring size and structure. Azaphenalene derivatives substituted with an amino group have low oxidation potentials and are easily reduced. Species such as these may be useful in the protection of biological systems from oxidative damage caused by reactive oxygen species, as the mechanism of protection is thought to include repeated oxidation and reduction of the nitroxide. Other families are expected to display less effective protection with piperidine, pyrrolidine, and isoindoline derivatives displaying higher oxidation potentials. Pyrrolidine and isoindoline derivatives also show more negative reduction potentials. Within a family of nitroxides, the variation of ring substituents have a smaller effect that generally follows the trends expected on the basis of electronegativity considerations, though the placement of a substituent around the ring is sometimes significant. Because the variation of substituents causes only minor modifications to the potential, it is expected that substituents can be chosen to affect the solubility or binding of a molecule without significantly compromising its antioxidant ability.

Acknowledgment. We gratefully acknowledge generous allocations of computing from the Australian Partnership for Advanced Computing and the Australian National University Supercomputing Facility, support from the Australian Research Council under their Centres of Excellence program, and the award (to J.L.H.) of an Australian Postgraduate Award.

Supporting Information Available: B3-LYP/6-31G(d) optimized geometries in the form of GAUSSIAN archive entries. This material is available free of charge via the Internet at <http://pubs.acs.org>.

References and Notes

- (1) (a) McCord, J.; Fridovich, I. *J. Biol. Chem.* **1969**, *244*, 6049. (b) Fridovich, I. *J. Biol. Chem.* **1989**, *264*, 7761.
- (2) Samuni, A.; Krishna, M. C.; Riesz, P.; Finkelstein, E.; Russo, A. *J. Biol. Chem.* **1988**, *263*, 17921.
- (3) Krishna, M. C.; Grahame, D. A.; Samuni, A.; Mitchell, J. B.; Russo, A. *Proc. Natl. Acad. Sci. U.S.A.* **1992**, *89*, 5537.
- (4) Krishna, M. C.; DeGraff, W.; Hankovszky, O. H.; Sár, C. P.; Kálai, T.; Jekó, J.; Russo, A.; Mitchell, J. B.; Hideg, K. *J. Med. Chem.* **1998**, *41*, 3477.
- (5) Winget, P.; Cramer, C. J.; Truhlar, D. G. *Theor. Chem. Acc.* **2004**, *112*, 217.
- (6) (a) Reynolds, C. A.; King, P. M.; Richards, W. G. *Nature* **1988**, *334*, 80. (b) Reynolds, C. A. *J. Am. Chem. Soc.* **1990**, *112*, 7545.
- (7) Fish, J. R.; Swarts, S. G.; Sevilla, M. D.; Malinski, T. *J. Phys. Chem.* **1988**, *92*, 3745.
- (8) See for example Namazian, M.; Almodarresieh, H. A.; Noorbala, M. R.; Zare, H. R. *Chem. Phys. Lett.* **2004**, *396*, 424.
- (9) Wass, J. R. T. J.; Ahlberg, E.; Panas, I.; Schiffrin, D. J. *J. Phys. Chem. A* **2006**, *110*, 2005.
- (10) Fu, Y.; Yu, H.-Z.; Wang, Y.-M.; Guo, Q.-X. *J. Am. Chem. Soc.* **2005**, *127*, 7227.
- (11) Kato, Y.; Shimizu, Y.; Yijing, L.; Unoura, K.; Utsumi, H.; Ogata, T. *Electrochim. Acta* **1995**, *40*, 2799.
- (12) Israeli, A.; Patt, M.; Oron, M.; Samuni, A.; Kohen, R.; Goldstein, S. *Free Radical Biol. Med.* **2005**, *38*, 317.
- (13) Hehre, W. J.; Radom, L.; Schleyer, P. V. R.; Pople, J. A. *Ab Initio Molecular Orbital Theory*; Wiley: New York, 1986.
- (14) Koch, W.; Holthausen, M. C. *A Chemist's Guide to Density Functional Theory*; Wiley-VCH: Weinheim, 2000.
- (15) Frisch, M. J.; Trucks, G. W.; Schlegel, H. B.; Scuseria, G. E.; Robb, M. A.; Cheeseman, J. R.; Montgomery, J. A., Jr.; Vreven, T.; Kudin, K. N.; Burant, J. C.; Millam, J. M.; Iyengar, S. S.; Tomasi, J.; Barone, V.; Mennucci, B.; Cossi, M.; Scalmani, G.; Rega, N.; Petersson, G. A.; Nakatsuji, H.; Hada, M.; Ehara, M.; Toyota, K.; Fukuda, R.; Hasegawa, J.; Ishida, M.; Nakajima, T.; Honda, Y.; Kitao, O.; Nakai, H.; Klene, M.; Li, X.; Knox, J. E.; Hratchian, H. P.; Cross, J. B.; Adamo, C.; Jaramillo, J.; Gomperts, R.; Stratmann, R. E.; Yazyev, O.; Austin, A. J.; Cammi, R.; Pomelli, C.; Ochterski, J. W.; Ayala, P. Y.; Morokuma, K.; Voth, G. A.; Salvador, P.; Dannenberg, J. J.; Zakrzewski, V. G.; Dapprich, S.; Daniels, A. D.; Strain, M. C.; Farkas, O.; Malick, D. K.; Rabuck, A. D.; Raghavachari, K.; Foresman, J. B.; Ortiz, J. V.; Cui, Q.; Baboul, A. G.; Clifford, S.; Cioslowski, J.; Stefanov, B. B.; Liu, G.; Liashenko, A.; Piskorz, P.; Komaromi, I.; Martin, R. L.; Fox, D. J.; Keith, T.; Al-Laham, M. A.; Peng, C. Y.; Nanayakkara, A.; Challacombe, M.; Gill, P. M. W.; Johnson, B.; Chen, W.; Wong, M. W.; Gonzalez, C.; Pople, J. A. *Gaussian 03*, revision B.03; Gaussian, Inc.: Pittsburgh, PA, 2003.
- (16) Werner, H.-J.; Knowles, P. J.; Amos, R. D.; Bernhardsson, A.; Berning, A.; Celani, P.; Cooper, D. L.; Deegan, M. J. O.; Dobbyn, A. J.; Eckert, F.; Hampel, C.; Hetzer, G.; Korona, T.; Lindh, R.; Lloyd, A. W.; McNicholas, S. J.; Manby, F. R.; Meyer, W.; Mura, M. E.; Nicklass, A.; Palmieri, P.; Pitzer, R.; Rauhut, G.; Schütz, M.; Stoll, H.; Stone, A. J.; Tarroni, R.; Thorsteinsson, T. *MOLPRO 2000.6*; University of Birmingham: Birmingham, 1999.
- (17) Curtiss, L. A.; Raghavachari, K. *Theor. Chem. Acc.* **2002**, *108*, 61.
- (18) Henry, D. J.; Sullivan, M. B.; Radom, L. *J. Chem. Phys.* **2003**, *118*, 4849–4860.
- (19) Vreven, T.; Morokuma, K. *Theor. Chem. Acc.* **2003**, *109*, 125.
- (20) Izgorodina, E. I.; Coote, M. L. *J. Phys. Chem. A* **2006**, *110*, 2486.
- (21) Izgorodina, E. I.; Brittan, D. B. R.; Hodgson, J. L.; Krenske, E. H.; Lin, C. Y.; Namazian, M.; Coote, M. L. *J. Phys. Chem. A* **2007**, *111*, 10754.
- (22) (a) Cancès, M. T.; Mennucci, B.; Tomasi, J. *J. Chem. Phys.* **1997**, *107*, 3032. (b) Cossi, M.; Barone, V.; Mennucci, B.; Tomasi, J. *Chem. Phys. Lett.* **1998**, *286*, 253. (c) Mennucci, B.; Tomasi, J. *J. Chem. Phys.* **1997**, *106*, 5151.

- (23) (a) Barone, V.; Cossi, M. *J. Phys. Chem. A* **1998**, *102*, 1995. (b) Cossi, M.; Rega, N.; Scalmani, G.; Barone, V. *J. Comput. Chem.* **2003**, *24*, 669.
- (24) Frisch, A.; Frisch, M. J.; Trucks, G. W. *Gaussian 03 User's Reference*; Gaussian, Inc.: Wallingford, CT, 2003.
- (25) Dutton, A. S.; Fukuto, J. M.; Houk, K. N. *Inorg. Chem.* **2005**, *44*, 4024.
- (26) Scott, A. P.; Radom, L. *J. Phys. Chem.* **1996**, *100*, 16502.
- (27) Siri, D.; Gaudel-Siri, A.; Tordo, P. *J. Mol. Struct. (THEOCHEM)* **2002**, *582*, 171.
- (28) Morishima, I.; Yoshikawa, K.; Yonezawa, T.; Matsumoto, H. *Chem. Phys. Lett.* **1972**, *16*.
- (29) Patterson, E. V.; Cramer, C. J.; Truhlar, D. G. *J. Am. Chem. Soc.* **2001**, *123*, 2025.

- (30) Namazian, M.; Siahrostami, S.; Noorbala, M. R.; Coote, M. L. *J. Mol. Struct. (THEOCHEM)* **2006**, *759*, 245.
- (31) Goldstein, S.; Samuni, A.; Hideg, K.; Merenyi, G. *J. Phys. Chem. A* **2006**, *110*, 3679.
- (32) Liptak, M. D.; Shields, G. C. *J. Am. Chem. Soc.* **2001**, *123*, 7314.
- (33) Bolton, R.; Gillies, D. G.; Sutcliffe, L. H.; Wu, X. *J. Chem. Soc., Perkin Trans. 2* **1993**, *11*, 2049.
- (34) Shen, J.; Bottle, S.; Khan, N.; Grinberg, O.; Reid, D.; Micallef, A.; Shartz, H. *Appl. Magn. Reson.* **2002**, *22*, 357.
- (35) Blinco, J. P.; McMurtrie, J. C.; Bottle, S. E. *Angew. Chem.* **2007**, *submitted*.